Redox Chemistry of Ca-Transporter 2-Palmitoylhydroquinone in an Artificial Thin Organic Film Membrane

Valentin Mirčeski,*,† Rubin Gulaboski,‡ Ivan Bogeski,§ and Markus Hoth§

Institute of Chemistry Faculty of Natural Sciences and Mathematics, Ss Cyril and Methodius University, Skopje, Republic of Macedonia, Faculdade de Ciências, Universidade do Porto, Rua do Campo Alegre, 687, 4169-007 Porto, Portugal, and Department of Physiology, Saarland University, 66421 Homburg, Germany

The redox chemistry of 2-palmitoylhydroquinone (H_2Q), a recently introduced synthetic transmembrane Ca^{2+} transporter, was studied with cyclic and square-wave voltammetry in an artificial thin organic-film membrane sandwiched between a pyrolytic graphite electrode and an aqueous solution. The membrane has a micrometer dimension and consists of the water immiscible organic solvent nitrobenzene, which contains suitable electrolyte and H_2Q as a redox active compound. The potential drop at the electrode/membrane interface is controlled by the potentiostat, whereas the potential drop at the membrane/water interface is dependent on the ClO_4^- concentration, which is present in a large excess in both liquid phases. The redox transformation of H_2Q at the electrode/membrane interface is accompanied by a corresponding ion-transfer reaction at the other side of the membrane. Proton transfer at the membrane/water interface is critical for the redox transformation of H_2Q in the interior of the membrane, as a strong dependence of the voltammetric response on the pH of the aqueous medium was observed. H_2Q undergoes two oxidation processes due to existence of two distinctive redox forms of H_2Q. The electrochemical mechanism can be explained with two tautomer forms of H_2Q formed by migration of a proton between the 1-hydroxyl group and the adjacent carbonyl group of the palmitoyl residue. Both tautomers undergo $2e/2H^+$ distinctive redox transformations to form the quinone form of the studied compound. In the presence of Ca^{2+} in the aqueous phase, voltammetric experiments confirmed the capability of both tautomers to form 1:1 complexes with Ca^{2+} and to extract it into the organic membrane. Upon the oxidation of the complexes, Ca^{2+} is expelled back to the aqueous phase. The studied compound exhibits very similar complexing affinity toward Mg^{2+}, implying that it is not highly selective for transmembrane Ca^{2+} transport.

1. Introduction

Organic compounds containing a benzoquinone/hydroquinone moiety are subjects of longstanding research efforts in various scientific areas due to their high relevance to biochemical systems. The most important example is ubiquinone-10 (also called coenzyme Q), which plays a critical role in the respiratory chain of mitochondria.[1] Embedded in the inner mitochondria membrane, ubiquinone-10 serves as an electron shuttle and a proton pump, generating a proton and potential gradient at the inner mitochondrion membrane. The energy conserved in a form of a potential gradient is further used for synthesis of adenosine-triphosphate. The redox chemistry of the quinone/hydroquinone system is essential for antioxidant activity of various compounds including several vitamins. For instance, vitamin E, which is incorporated in cell membranes, acts as a scavenger for free radicals and reactive oxygen species. On the other hand, vitamin K, another quinone derivative, is crucial for the blood coagulation process. Quinones/hydroquinones redox chemistry is also involved in photosynthesis in which hydroquinones operate as reducing agents mediating various processes that finally lead to oxygen release.

Electrochemical techniques are very well suited for characterizing quinone-like compounds.[2-9] As most of the physiologically active quinones are lipophilic, electrochemical methods in nonaqueous medium have been developed.[4,6,8] Particularly important are biomimetic studies in which lipophilic quinone is embedded in a lipid membrane supported on the electrode surface.[3] Liposomes are also suitable for membrane immobilization of lipophilic quinones. In this context, Bennett et al.[10] have recently incorporated the synthetic 2-palmitoylhydroquinone (H_2Q) in a liposome membrane to build an artificial light-driven transmembrane calcium pump. Although the redox chemistry of H_2Q is hardly known, these authors have utilized its redox sensitivity to analyze binding of Ca^{2+}. According to their work, H_2Q is recommended as a selective commercially available membrane transporter of Ca^{2+} ions. The remarkable work of Bennett et al. points out that the redox chemistry of the benzoquinone/hydroquinone system is not only important for biochemical electron-transfer chains, but it can play a crucial role in the redox sensitive transmembrane transport mechanisms of metal cations. Ca^{2+} is extremely relevant in this context because Ca^{2+} transport across membranes is one of the most important signaling mechanisms in basically all cells.[11]

In the current study, we directly probe the redox properties of H_2Q (Figure 1) by means of thin-film electrodes in connection with voltammetric techniques. The aim of the present work is to provide an insight into the redox chemistry of this important

---

 * To whom correspondence should be addressed. E-mail: valentin@iunona.pmf.ukim.edu.mk.
 † Ss Cyril and Methodius University.
 ‡ Universidade do Porto.
 § Saarland University.

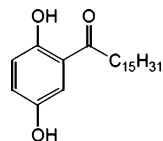Ca^{2+} and Proton Transfer Across Artificial Membranes

J. Phys. Chem. C, Vol. 111, No. 16, 2007 **6069**

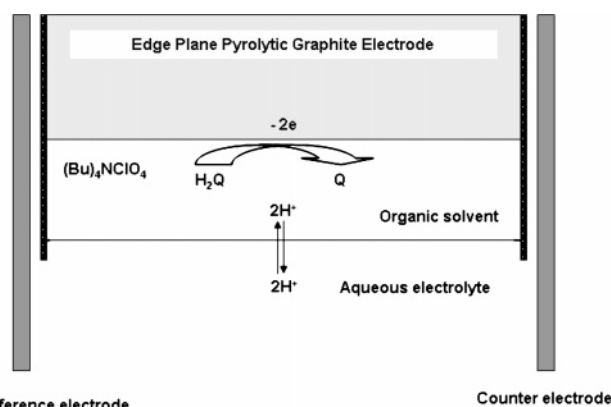**Figure 1.** Molecular structure of 2-palmitoylhydroquinone.

Figure 2. Schematic representation of the thin-film electrode assembly consisting of a membrane of an organic solvent imposed on the graphite electrode surface. The membrane contains H$_2$Q as a redox probe and a suitable electrolyte. The thin-film electrode is immersed into aqueous-buffered solution containing a common ion with the organic electrolyte. The modified electrode is used in a conventional three-electrode configuration.

lipophilic synthetic compound embedded in an artificial membrane, as well as to probe its capabilities to facilitate the transport of Ca^{2+}, Mg^{2+}, and Ba^{2+} across water/organic-film membrane interface.

The experimental assembly used (Figure 2) consists of a micrometer dimension organic-film membrane sandwiched between a highly oriented pirolytic graphite electrode and an aqueous electrolyte solution. The organic-film membrane consists of a water immiscible nitrobenzene (NB) solution containing a suitable electrolyte and H$_2$Q as a redox active compound. The membrane forms a stable liquid interface with the aqueous phase, whereas its high electrical conductance and partial water content permit ionic and protolitic reactions to proceed at an appreciable rate in the membrane interior. H$_2$Q, which is present at millimolar concentration levels, undergoes redox transformation at the electrode/membrane interface, the redox transformation being driven by the potential gradient controlled by potentiostat. The potential drop at the membrane/water interface is dependent on the distribution of ClO$_4^-$, which is present in large excess in both liquid phases. The electron transfer at the one side of the membrane is accompanied by a simultaneous charge compensating ion-transfer reaction at the other side of the membrane. The overall electrochemical process couples the electron with the ion-transfer reaction proceeding at different membrane sides. Thus, the experimental system used, though quite simple, provides an insight into the mechanistic, energetic, and kinetic features of the coupled electron−ion-transfer reaction of biochemical significance.[12−18]

The electrochemical experiments have been conducted with conventional cyclic (CV)[19] and square-wave voltammetry (SWV)[20] techniques. The latter technique is one of the most advanced voltammetric methods unifying the advantages of CV and pulse voltammetric techniques. In the course of a SW voltammetric experiment, the potential is repeatedly changed to an oxidative and reductive mode in a form of square-shaped potential pulses. The time interval in which a redox reaction is completed in both oxidation and reduction directions ranges
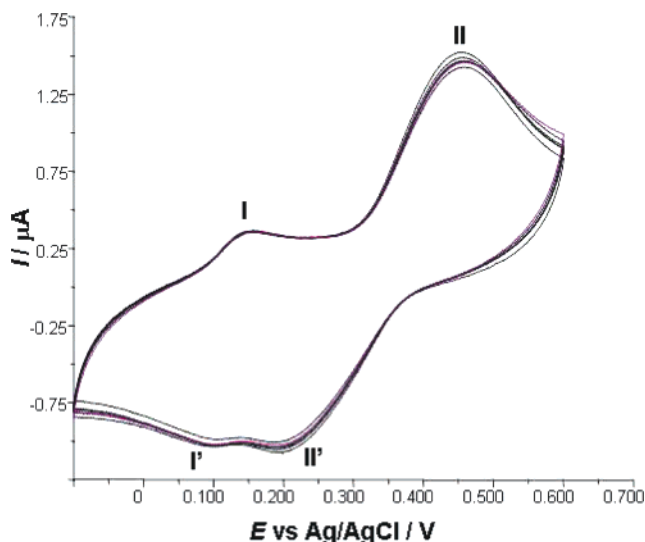

Figure 3. Consecutive cyclic voltammograms recorded at the thin-film electrode containing 10 mol/L H$_2$Q in contact with 0.1 mol/L KClO$_4$ aqueous solution buffered with a 0.1 mol/L phosphate buffer at pH of 5.0. Besides the redox probe, the organic phase contains 0.1 mol/L tetrabuthylammonium perchlorate (Bu$_4$NClO$_4$) as an organic electrolyte. Scan rate was v = 5 mV/s.

from 1 to 100 ms, thus providing intrinsic information on the charge-transfer mechanism and kinetics of the studied electrochemical reaction.

2. Materials and Methods

H$_2$Q (99% purity) was purchased from MERCK and was used without further purification. All other chemicals were of highest purity. H$_2$Q was dissolved in a water-saturated NB at a concentration of 10 mmol/L. Besides the redox compound, NB contained 0.1 mol/L tetrabuthylammonium perchlorate (Bu$_4$NClO$_4$) as an organic electrolyte. A disk electrode (0.32 cm^2) of edge plane pyrolytic graphite (EPGE) was used as a working electrode. An Ag/AgCl (3 M KCl) electrode was used as a reference and a platinum wire as an auxiliary electrode. The modification of the working electrode and its pretreatment is described elsewhere.[17] NB solution (0.5 μL) was deposited on the graphite electrode with the help of a micropipette; the organic solution spreads spontaneously over the electrode surface forming a stable film. The modified electrode was immersed into aqueous buffer solutions composed of 0.1 mol/L Na$_2$HPO$_4$, 0.1 mol/L NaH$_2$PO$_4$, and an appropriate amount of citric acid. Besides the buffer, the aqueous phase contained 0.1 mol/L KClO$_4$ as a supporting electrolyte. NB-saturated water (Millipore Q) was used for preparing all aqueous solutions.

In addition, electrochemistry of microcrystals of H$_2$Q-immobilized on the electrode surface was also studied in a direct contact with the aqueous phase. To achieve this, 0.5 μL of a dichloroethane solution of H$_2$Q (c = 10 mmol/L) was imposed on the electrode surface. After evaporation of the solvent for a few minutes, the surface of EPGE had been modified with immobilized microcrystals of H$_2$Q.

SW and cyclic voltammograms were recorded using μAutolab Model III equipment (Eco-Chemie, Utrecht, Netherlands). All experiments were performed at room temperature.

3. Results

3.1. Redox Behavior of H$_2$Q in the Organic-Film Membrane in Contact with Ca^{2+}-Free Aqueous Solutions. Shown in Figure 3 are typical CVs of H$_2$Q embedded in a NB
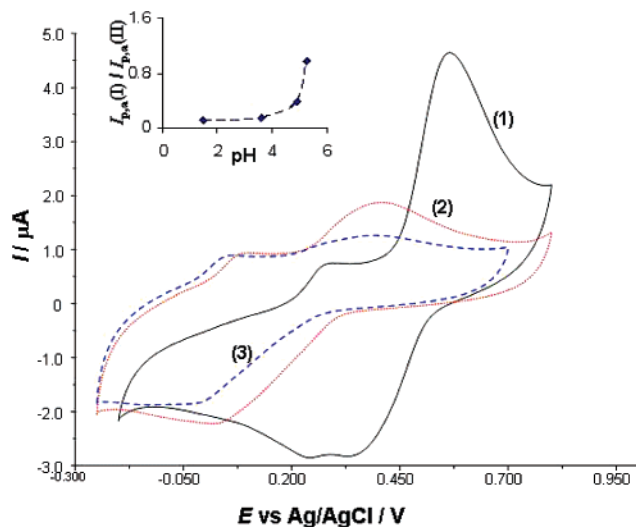
Figure 4. Cyclic voltammograms at thin-film electrode recorded in contact with aqueous medium at pH 1.5 (1), 4.9 (2) and 5.3 (3). Scan rate was 10 mV/s. The other conditions are the same as for Figure 3. The inset shows the dependence of the anodic peak current ratio $I_{p,a}(I)/I_{p,a}(II)$ on pH.

membrane in contact with an aqueous buffer at pH of 5, recorded by consecutive cycling of the potential. The features of repetitive CVs reflect the stability of the membrane and the chemical reversibility of the redox transformations of H_2Q. CV response of H_2Q features two distinctive peak-pairs (i.e., I–I′ and II–II′). The relative heights and positions of the voltammetric peaks are strongly sensitive to the pH, which was varied from 1 to 7; at higher pH the voltammetric parameters of the CV response were hardly measurable. Figure 4 shows typical CVs recorded at $v = 10$ mV/s at different pH. The midpeak potentials ($E_{p,m} = (E_{p,a} - E_{p,c})/2$ in which $E_{p,a}$ and $E_{p,c}$ correspond to the peak potential of the anodic and cathodic peak, respectively) of both redox processes shift linearly with pH (data not shown) with a slope of about −60 mV/pH, indicating that the two oxidation processes of H_2Q are accompanied by an expulsion of protons from the membrane into the aqueous phase. The inset of Figure 4 presents the variation of the anodic peak current ratio $I_{p,a}(I)/I_{p,a}(II)$, which was increased from 0.11 to 0.97 if the pH was increased from 1.5 to 5. Higher pH increased the amplitude of first oxidation peak at the expense of the second one. Moreover, an increase of pH caused a strong shift of the cathodic peak II′ toward more negative potentials. The voltammetric curve 2 in Figure 4 shows that the latter cathodic peak appears only as a shoulder of the cathodic peak I′, whereas at pH 5.3 (curve 3) the cathodic peak II′ is completely merged into the cathodic peak I′.

The peak potential separation of the peak-couple I–I′ depended mainly on the scan rate. At a low scan rate of $v = 1$ mV/s, the peak potential separation is 40 and 42 mV for an aqueous medium at pH 5 and 1.5, respectively, being close to the theoretical value of 30 mV for a reversible two-electron process.[19] An increase of the scan rate up to $v = 100$ mV/s was followed by a permanent increase of the potential separation of the couple I–I′, which is typical for a quasireversible electrode process. At pH 5, the potential separation at $v = 0$ mV/s, found by extrapolation of the dependence E_p versus v for the peaks I and I′, is about 38 mV (see the inset of Figure 5a). On the other hand, the voltammetric behavior of the peak couple II–II′ is considerably different. For the same voltammograms mentioned above, recorded at pH 1.5 and 5 at $v = 1$ mV/s, the peak potential separation for the couple II–II′ is 101

and 128 mV, respectively. The peak potential separation of the couple II–II′ increased more rapidly by increasing the scan rate compared to the couple I–I′. Moreover, the peak potential separation increased significantly by increasing of pH of the medium (see Figure 5), which was much less pronounced for the couple I–I′.

The evolution of the CVs as a function of the scan rate at a constant pH is shown in Figure 5. The inset of Figure 5b shows the variation of the peak current ratio $I_{p,a}(I)/I_{p,a}(II)$ by increasing the scan rate. In addition, the cathodic peak II′ strongly shifted toward negative potentials by increasing the scan rate. Indeed, this peak disappeared, or it was merged into the cathodic peak I′, for a scan rate $v \geq 100$ mV/s (Figure 5d). Obviously the effect of the scan rate on the peak current ratio and the position of the cathodic peak II′ is equivalent to that of pH, shown in Figure 4. The inset of Figure 5c shows the variation of the scan rate-normalized anodic peak current, $I_{p,a}/v$ versus v, for both anodic peaks I and II. The ratio I_p/v for anodic peak II decreases severely by increasing the scan rate, indicating a CE mechanism in which the electrode reaction is gated by a slow-preceding chemical step.[19]

The response of H_2Q in the NB membrane under conditions of SWV consisted of two well-defined and separated oxidative net peaks (Figure 6A). At a constant pH, the relative heights of the two peaks varied proportionally with the number of repetitive SW voltammograms recorded with a single thin-film electrode. The evolution of consecutive SW voltammograms reveals that the magnitude of the peak I increases in proportion with the time of subsequent SW potential cycling, whereas peak II proportionally diminishes (Figure 6A). The sum of both peaks is virtually constant for each voltammogram, while a steady-state response is reached after 5 min of potential cycling (see the inset of Figure 6A). Interestingly, without potential cycling the peak heights were insensitive to the contact time of the electrode with the aqueous electrolyte (Figure 6B). If the resting potential was kept at the value between the peaks I and II (i.e., $E_{rest} = 0.15$ V), the duration of the resting period had no effect on the magnitude of the peak II, indicating that the electroactive reactant for the process II is not generated during the electrode process I (Figure 7).

To probe the redox chemistry of H_2Q in direct contact with the aqueous phase, microcrystals of H_2Q were immobilized on the EPGE, applying the procedure described in Section 2. The response of H_2Q microcrystals immobilized on the electrode surface consisted of two well-separated SW peaks (Figure 8A). The position of the response was strongly sensitive to the pH of the aqueous phase. Moreover, the ratio $I_p(I)/I_p(II)$ increased by increasing pH, as well as by repetitive cycling of the potential in the SWV experiment. Overall, the intrinsic voltammetric behavior was similar to that observed in a thin-film experiment.

The variation of the frequency provides further insight into the electrode mechanisms of the two processes. As shown in Figure 8B, the net peak current I increased nonlinearly with the frequency, which is typical behavior for quasireversible processes of an immobilized reactant[20] or a reactant embedded in a thin-film membrane.[21] On the contrary, the peak II strongly diminished as the critical time of the voltammetric experiment was decreased (i.e., by increasing the frequency). The diminishing of the peak II is typical for both the microcrystal-modified electrode and for the thin-film electrode assembly. This analysis strongly suggests a CE reaction scheme for the process II, which agrees with the results observed with CV (cf. Figure 5c). It should be noted that the decrease of the peak II is more
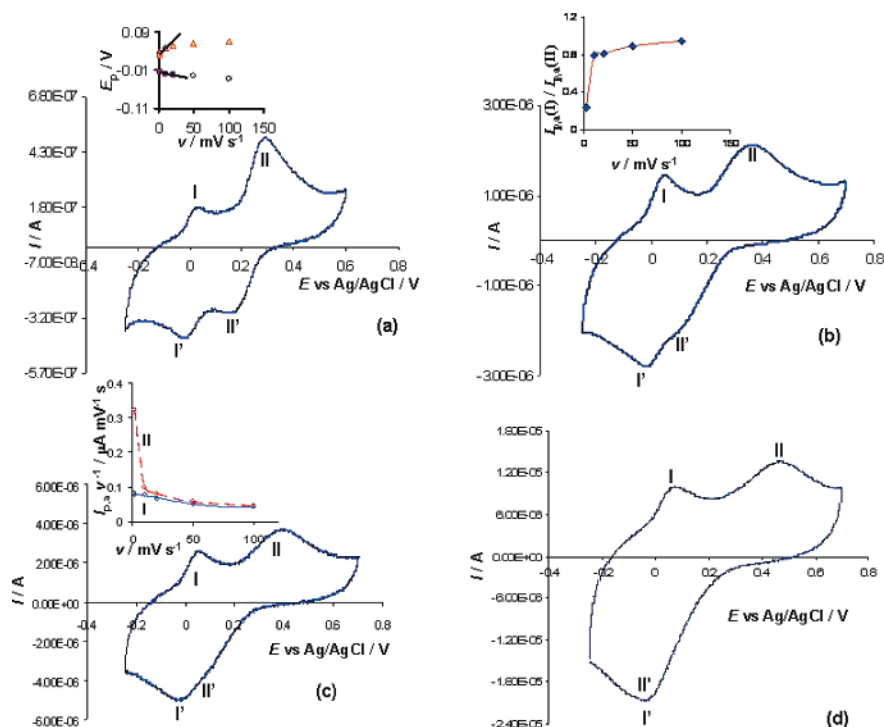
Figure 5. Effect of the scan rate on the shape of the cyclic voltammograms recorded at thin-film electrode in contact with an aqueous medium at pH 5. The scan rate was $v = 1$ (a), 10 (b), 20 (c), and 100 mV/s (d). The inset of (a) shows the variation of the peak potential with the scan rate for the peaks I and I′. The inset of (b) shows the variation of the anodic peak current ratio $I_{p,a}(I)/I_{p,a}(II)$ on the scan rate. The inset of (c) shows the variation of the ratio $I_{p,a}/v$ on the scan rate for the peaks I and II.

pronounced under conditions of SWV than in CV, as the former is the much faster voltammetric method.

The kinetics of the electrochemical process I were further analyzed by exploiting the "quasireversible maximum" (QRM) phenomenon, a feature typical for surface processes[20] and processes in thin-film membranes.[18,21,22] The theoretical background of this methodology has been elaborated in a series of previous publications.[16,18,21,22] The theory predicts a parabolic dependence of the ratio $I_p f^{-0.5}$ versus f (or alternatively, log-(f)) with the maximum of the parabola being located within the quasireversible kinetic region of the studied redox reaction in the membrane. The exact position of the QRM is associated with a certain critical frequency (f_{max}) upon which the rate of the redox transformation is synchronized with the frequency thus producing a maximum ratio $I_p f_{max}^{-0.5}$. The faster the kinetics of the studied reaction is, the higher the critical frequency is. For complex processes in a thin-film membrane in which the electron transfer at one side is coupled with the ion transfer at the other side of the membrane, the features of the QRM allow the detection of the of the rate-limiting step of the overall electrochemical reaction. For instance, when the ion transfer is the rate decisive step, the position of the QRM shifts consistently toward higher critical frequencies by increasing the concentration of the transferring ion in the aqueous phase.[16,22]

When the electrode was modified with microcrystals of H₂Q, a well-formed QRM was observed with a position of the maximum being dependent on pH of the medium. Decreasing pH caused the maximum to shift toward higher frequencies, the critical values being f_{max} = 60 and 320 Hz for pH 3.9 and 1.5, respectively. An analogous behavior of the QRM was observed for the experiment in a thin membrane in which the corresponding critical frequencies are f_{max} = 30 and 280 Hz for pH 3.9 and 1.5, respectively. It should be noted that in the thin-film experiment the redox transformation in the membrane must be accompanied by a corresponding ion-transfer reaction

across the water/membrane interface to maintain the charge neutrality of the membrane. To analyze the influence of the ion-transfer reaction on the overall electrochemical process in the membrane, kinetic measurements have been conducted by systematic alteration of the potential drop at the water/membrane interface. These experiments have been performed by adjusting the concentration of ClO_4^- in both liquid phases, which is the main potential-controlling ion present in a large excess in both liquid phases. Figure 9 shows the evolution of the QRM by increasing the ClO_4^- concentration in the aqueous phase, which is manifested as an acceleration of the overall redox transformation within the membrane.

3.2. Redox Behavior of H₂Q in Aqueous Solutions Containing Ca²⁺ Ions. Ca²⁺, as a double-charged ion, exists as a strongly hydrated ion in an aqueous medium. In a medium with pH > 7, hydroxo-complexes of Ca²⁺ are also encountered. The hydrophobicity of Ca²⁺ is so high that its direct transfer from aqueous to nonaqueous medium cannot be achieved with the contemporary electrochemical techniques. For these reasons, the transfer of Ca²⁺ ions across artificial or living cell membranes proceeds according to a facilitated ion-transfer mechanism enabled by lipophilic-complexing agents embedded in the membrane. On the basis of this mechanism, H₂Q has been exploited as a Ca²⁺ transporter through liposome membrane.[10]

Figure 10A depicts several SW voltammograms recorded after the thin-film electrode was immersed in a buffer solution containing various concentrations of Ca²⁺ ions. As can be inferred from Figure 10A, the redox chemistry of H₂Q in the membrane is sensitive to the Ca²⁺ content in the aqueous phase. An increase of the Ca²⁺ concentration causes a proportional and equivalent shift of both voltammetric peaks toward more positive potentials. The dependence of the net peak potentials on the logarithm of the Ca²⁺ concentration is linear with an identical slope for both peaks of about 36 mV/log [Ca²⁺] (Figure 10B). Besides the position, the Ca²⁺ concentration significantly
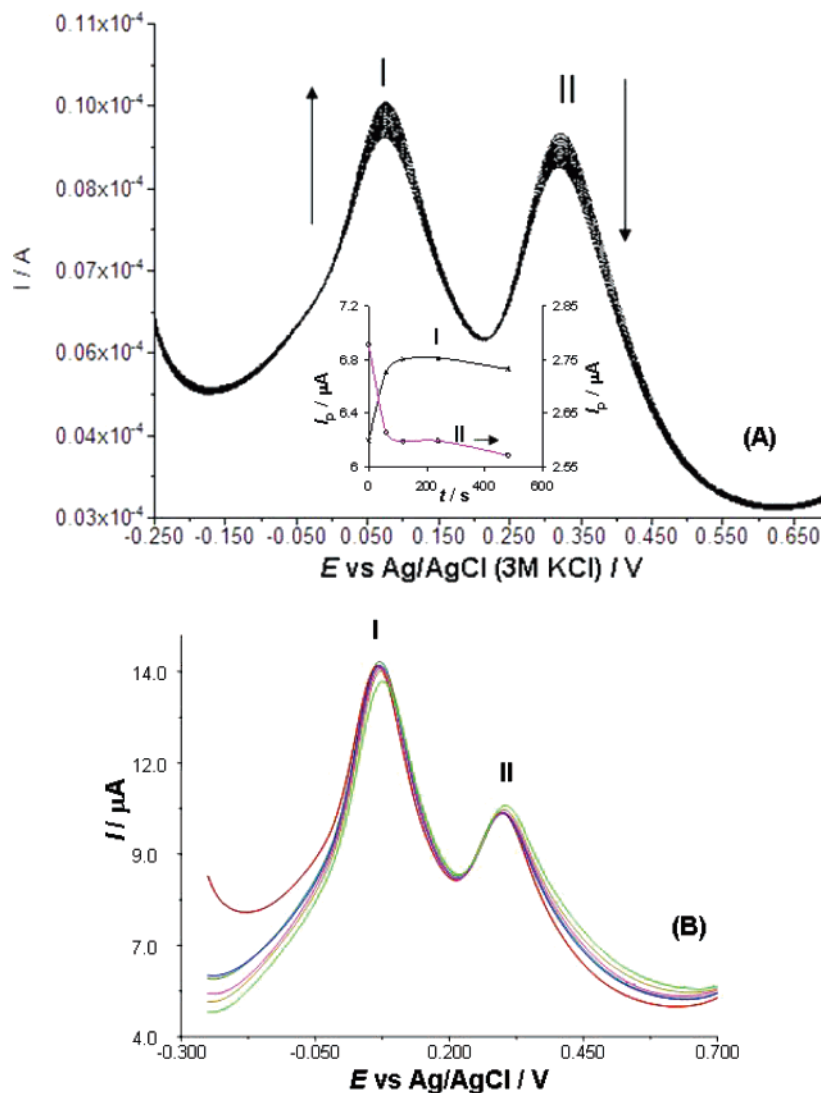
Figure 6. (A) Consecutive net SW voltammograms recorded at the thin-film electrode in contact with aqueous medium at pH 3.9. The inset shows the dependence of the net peak currents of peaks (I) and (II) on the time of potential cycling. (B) Effect of the resting time of the electrode in the aqueous electrolyte, varied from 0 to 1000 s with a step of 100 s. The resting potential was −0.25 V. Each voltammogram was recorded by imposing a new film on the electrode surface. The parameters of the potential modulation were: SW frequency f = 8 Hz, SW amplitude E_{sw} = 50 mV, and scan increment dE = 1 mV. The other conditions are the same as for Figure 3.

affected the magnitude of the voltammetric peaks. Enhancing the Ca^{2+} concentration resulted in a consistent enlarging of the peak I. At the same time, the peak II proportionally diminishes. It is very important to emphasize that the pH dependence of both processes is significantly altered in the presence of Ca^{2+}. For 9 mM Ca^{2+}, the linear dependence of E_p versus pH had a slope of −34 mV/pH for both redox processes. The corresponding dependence in the absence of Ca^{2+} was −60 mV/pH.

At a constant pH and Ca^{2+} concentration, the relative peak heights vary strongly with the contact time of the membrane with the aqueous phase with or without repetitive cycling of the SW potential modulation. This effect is clearly illustrated by the repetitive SW voltammograms shown in Figure 11A. The first peak strongly increased over time at the expense of the second one. After a period of 15 min, the second peak almost completely vanished. Note that similar behavior was observed in a Ca^{2+}-free aqueous solution (Figure 6A). However, in the absence Ca^{2+} ions, the overall effect was less pronounced, and the repetitive potential cycling led to a steady-state voltammogram without a complete vanishing of the peak II. Figure 11B shows the evolution of SW voltammograms with the incubation

time of the electrode in a separate aqueous solution containing 0.1 mol/L Ca^{2+} ions. After the incubation period, the electrode was transferred into a Ca-free buffer solution to record the voltammogram. Again, the first peak increased with time at the expense of the second one, which almost vanished after an incubation period of 45 min. This is a unique phenomenon related to the incubation in a Ca^{2+}-containing solution (compare Figures 6B and 11B).

Kinetic measurements carried out with QRM referring to the peak I showed that the apparent kinetics of the electrochemical process is independent of the content of Ca^{2+} ions in the aqueous phase. The binding and transferring abilities of H_2Q toward Mg^{2+} and Ba^{2+} ions were also tested. Figure 12 shows the evolution of the SW voltammograms at various concentrations of Mg^{2+} and Ba^{2+} ions. The overall voltammetric behavior in the presence of Mg^{2+} (Figure 12A) is equivalent to that in the presence of Ca^{2+} ions, revealing that H_2Q does not discriminate between Ca^{2+} and Mg^{2+} ions. On the contrary, the voltammetric response is insensitive to Ba^{2+} (Figure 12B), showing the absence of complexing ability of H_2Q toward these ions.

Ca^{2+} and Proton Transfer Across Artificial Membranes

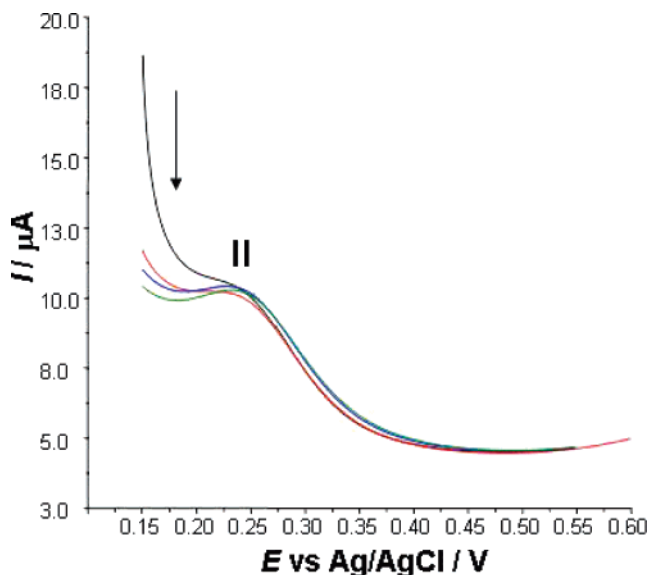*J. Phys. Chem. C, Vol. 111, No. 16, 2007* **6073**

Figure 7. Effect of the resting potential on the net SW peak II, recorded with a thin-film electrode in contact with an aqueous solution at pH 5. The resting potential was 0.15 V. The time increases in the direction of the arrow from 0, 20, 50, to 100 s. The other conditions are the same as for Figure 3. The parameters of the potential modulation are the same as for Figure 6.
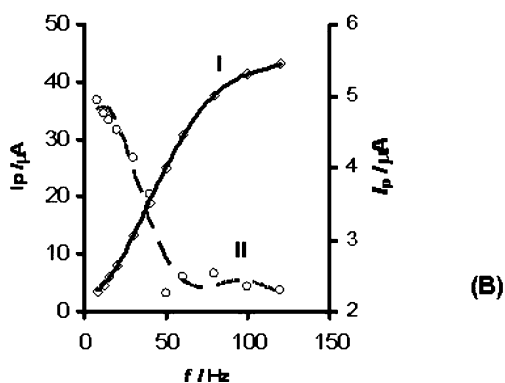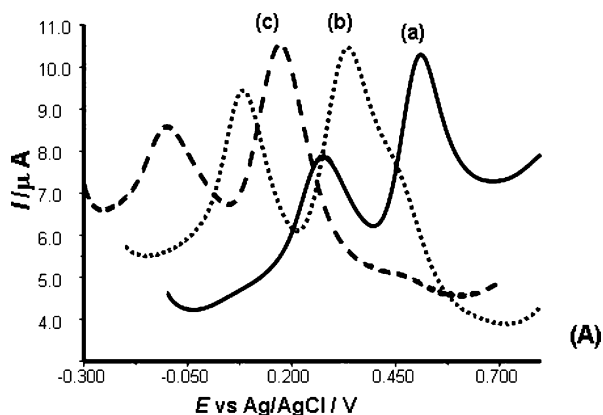

Figure 9. Quasireversible maxima corresponding to the redox process I recorded in contact with an aqueous solution at pH of 3.9 containing ClO$_4^-$ at a concentration of 0.9 (a), 10 (b), 30 (c), and 100 mmol/L (d). Parameters of the potential modulation were E_{sw} = 50 mV and dE = 1 mV. The other conditions are the same as for Figure 3.

Figure 8. (A) SW voltammetric responses of immobilized microcrystals of H$_2$Q recorded in direct contact with the aqueous phase at pH 1 (a), 3.9 (b), and 7 (c). The parameters of the potential modulation were the same as for Figure 6. (B) Dependence of the net SW peaks I and II on the frequency of the potential modulation for pH 3.9.

Figure 10. (A) SW voltammograms of thin-film electrode recorded in the presence of Ca^{2+} with the aqueous solution buffered to pH 3.9. The concentration of Ca^{2+} was 0, 5.8, 11.1, 15.3, and 19 mmol/L (from left toward right). The other conditions were same as for Figure 3. (B) Dependence of the peak potentials E_p on the log(Ca^{2+}) for both voltammetric peaks.

4. Discussion

The electrochemistry of benzoquinone/hydroquinone redox couple in both aqueous[2,3,5,7] and nonaqueous[4,6,8] mediums has been the subject of numerous investigations. In an aqueous medium, the general reaction scheme known as a scheme of
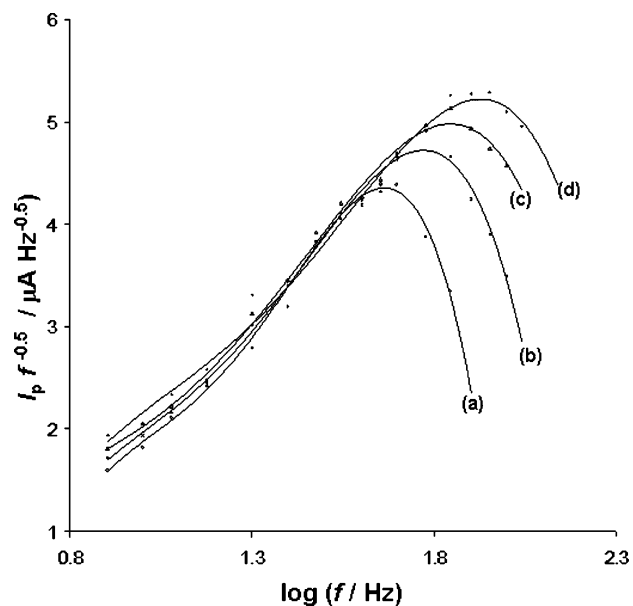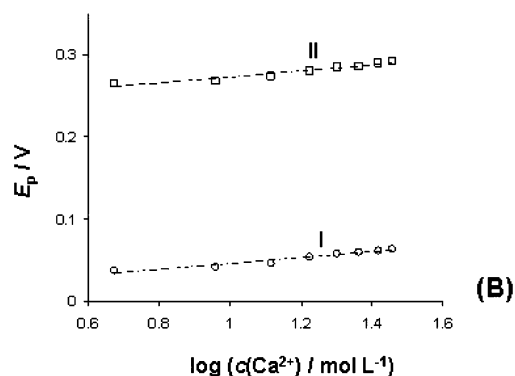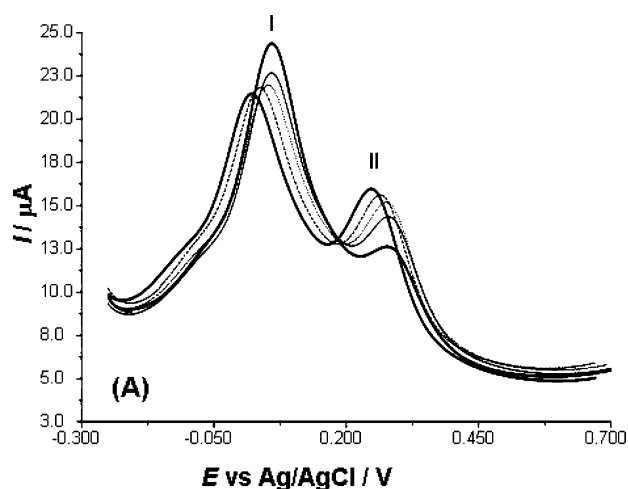
squares is particularly complicated, including six possible redox transformations coupled to six protonation reactions. Nevertheless, in an aqueous media the redox transformation most
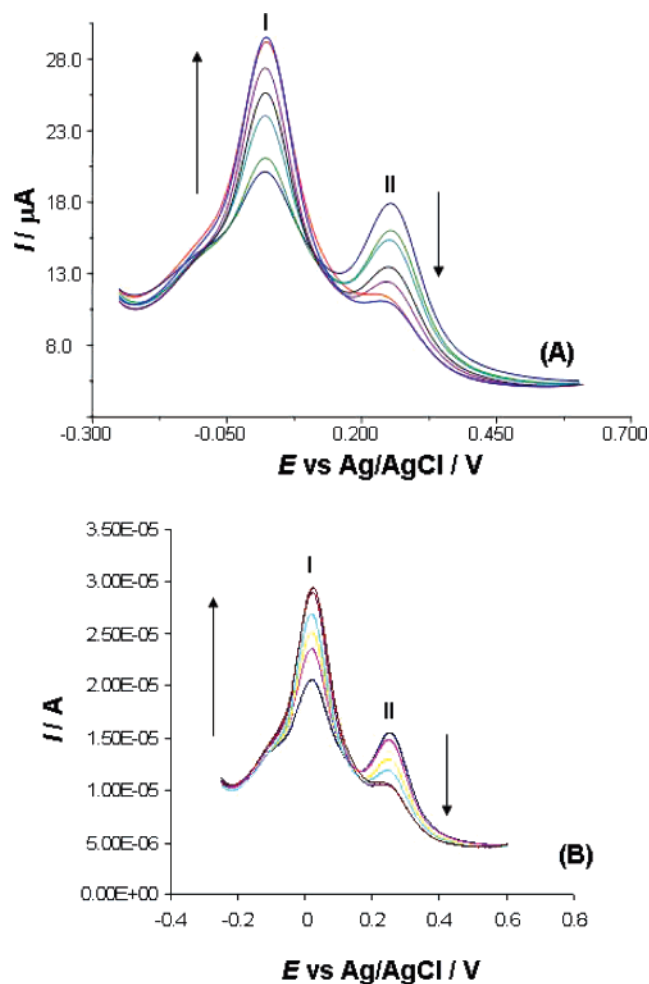
6074 *J. Phys. Chem. C, Vol. 111, No. 16, 2007*

Mirčeski et al.

Figure 11. (A) Consecutive net SW voltammograms recorded in contact with aqueous medium at pH 3.9 containing 5.8 mmol/L Ca^{2+}. (B) Effect of the incubation time of the electrode in a separate aqueous solution containing 0.1 mol/L Ca^{2+} ions. The incubation time increases in the direction of the arrows from 3, 7, 13, 21, 35, and 45 min. After incubation period, the electrode was transferred into a Ca^{2+}-free aqueous solution at pH 5.8. The other conditions are the same as in Figure 5.

Figure 12. SW voltammograms recorded in the presence of Mg^{2+} (A) and Ba^{2+} (B) ions in the aqueous phase at pH 5.0. For (A), the concentration of Mg^{2+} was 0, 10, 20, 30, and 40 mmol/L (from left to right). For (B), the concentration of Ba^{2+} was 0, 4.7, 9.3, 13.1, and 17 mmol/L. Parameters of the potential modulation were $f = 8$ Hz, $E_{sw} = 50$ mV, and $dE = 1$ mV. The other conditions are the same as for Figure 3.

frequently appears as a quasireversible one step, coupled two-electron-two-proton ($2e/2H^+$) process.[2] On the contrary, in a nonaqueous media, two energetically distinctive reversible one-electron redox steps have been observed with voltammetric techniques, mediated by formation of a semiquinone form.[2,3]

The overall voltammetric behavior of the studied compound strongly deviates from the common behavior of the benzoquinone/hydroquinone redox couple.[23] Voltammetric curves recorded under a variety of conditions feature two distinctive oxidative processes with strongly different voltammetric characteristics. The two processes are not exclusively observed in the thin organic-film membrane experiment, but they are equally present in the experiments conducted in direct contact with the aqueous phase. At a slow scan rate, the voltammetric features of the oxidative process I are close to the reversible behavior typical for a two-electron process (cf. Figure 5a). Taking the linear dependence on pH with a slope of −60 mV/pH into account, it follows that the oxidative process I involves overall $2e/2H^+$ exchange, which is typical for benzoquinone/hydroquinone redox couple. On the contrary, the process II exhibits typical characteristics of a CE reaction scheme in which the electroactive reactant is supplied by a preceding chemical reaction. This is confirmed by varying the scan rate in CV and
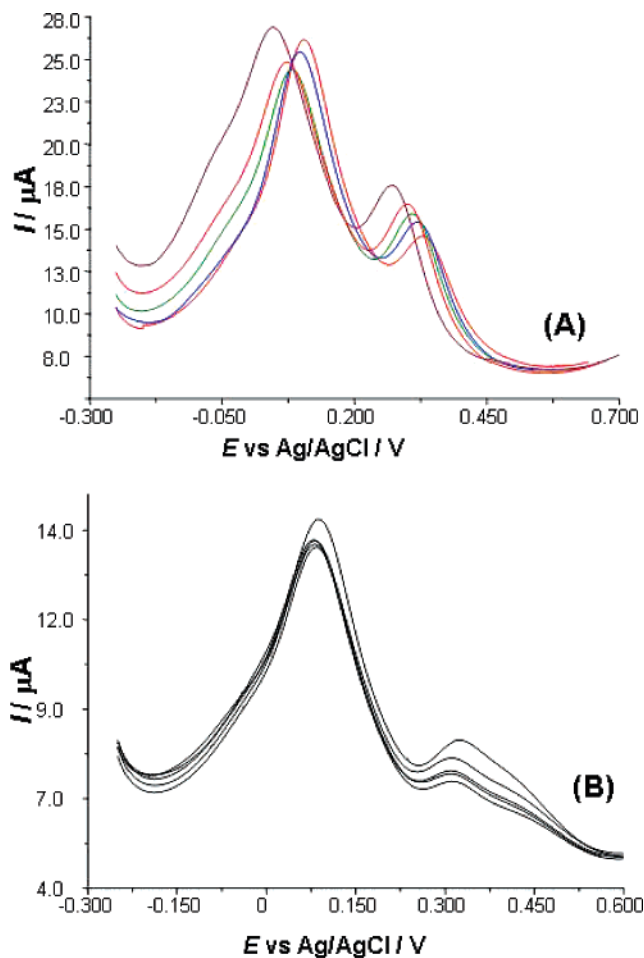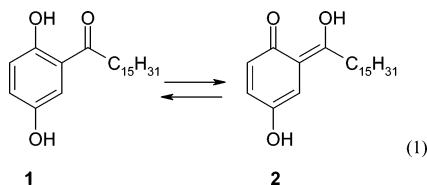
frequency in SWV for both types of experimental arrangements (cf. Figures 5c and 8B). Moreover, the results presented in Figure 7 show that the electroactive reactant for the oxidative process II is not generated in the previous electrochemical process I. This excludes the possibility to explain the two oxidative processes on the basis of two one-electron consecutive processes with a formation of a stable semiquinone radical. Furthermore, a careful inspection of the voltammetric curves in Figure 7 reveals that the current due to the second oxidative process II slightly decreases with time. Therefore, the two electrochemical processes originate from redox transformations of two distinctive redox forms of H_2Q molecule. The interrelation of the peak magnitudes implies that the two redox forms are interconnected by a chemical equilibrium reaction. Over a variety of experimental conditions, the sum of the two oxidative peaks is constant and proportional to the total concentration of H_2Q.

Considering the molecular structure of H_2Q (Figure 1), it is reasonable to assume that the intriguing voltammetric characteristic of the present compound originates from the influence of palmitoyl residue in the position 2 of the hydroquinone ring. The carbonyl group in the position 2 can establish a tautomerism equilibrium with the adjacent hydroxyl group from the hydroquinone ring as follows:[24]

Ca^{2+} and Proton Transfer Across Artificial Membranes

J. Phys. Chem. C, Vol. 111, No. 16, 2007 **6075**

(1)

Both tautomers **1** and **2** can undergo independent redox transformation to yield a quinone form according to the following schemes:


(2)

(3)
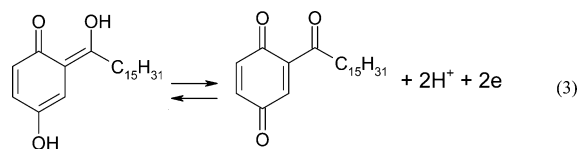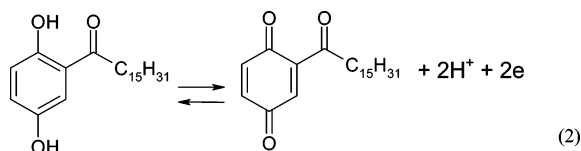
Reaction 2 is the common redox transformation of the hydroquinone/benzoquinone redox couple involving an overall 2e/2H$^+$ exchange, assigned to the oxidation process I. The equilibrium chemical reaction (1), coupled to the redox reaction (3), completes a CE reaction scheme thus being attributed to the oxidation process II.

The position of the tautomerism equilibrium 1 depends critically on the pH of the medium, being shifted toward the form **2** by decreasing pH, which agrees with the known acidic catalysis of the keton-enol transformation.[25] For these reasons, the ratio of the anodic peak currents $I_{p,a}(I)/I_{p,a}(II)$ increases with increasing pH (cf. Figure 4). The kinetics of the tautomer transformation is apparently a slow process, which causes a decrease of the net SW peak II by enhancing the SW frequency, as shown in Figure 8B. For the same reasons, the ratio $I_{p,a}(II)/v$ decreases (cf. Figure 5c), whereas the anodic peak current ratio $I_{p,a}(I)/I_{p,a}(II)$ increases (cf. Figure 5b) with an increased scan rate of the CV experiment. In addition, as can be inferred from the results in Figure 5, the redox reaction (3) is an electrochemically irreversible process. The kinetics of the reduction of the quinone form back to the tautomer form **2** are very low, depending critically on the pH of the medium. Accordingly, the increase of either the pH or the scan rate in a CV experiment caused the reduction peak II′ to shift strongly toward negative potentials. Obviously, at pH $\geq$ 5.5 and $v \geq$ 100 mV/s the reduction of quinone form yields mainly tautomer **1** (cf. Figures 4 and 5).

The slow establishment of the tautomer equilibrium explains the evolution of the SW voltammograms under the repetitive cycling of the SW potential modulation (cf. Figure 6A). During a SW potential scan, a part of both **1** and **2** forms of the previously established equilibrium is consumed, resulting in formation of the quinone form. Switching the potential to the initial value (i.e., −0.25 V) the form **1** is mainly generated without having sufficient time to re-establish the equilibrium 1. As a consequence, the oxidation peak I increases at the expense of the peak II. If the electrode was kept for a certain period in contact with the aqueous solution under open circuit conditions or at the initial potential value, the contact time had no effect on the shape of voltammograms, as the position of the tautomerism equilibrium was predominantly fixed by the pH of the medium (cf. Figure 6B).

The kinetic measurements conducted with QRM for both experimental configurations showed that the apparent rate of the reaction 2 increased by decreasing the pH, agreeing with theoretical predictions for this type of redox processes.[2,23] For the thin-film experiment, the situation is particularly complex as the 2e/2H$^+$ redox transformation in the membrane must be accompanied by a corresponding ion-transfer reaction across the membrane/water interface to maintain the charge neutrality of the membrane. If the proton expulsion is the charge-compensating ion-transfer reaction, the reaction 2 should be written as follows:

$$H_2Q_{(nb)} \rightleftharpoons Q_{(nb)} + 2H^+_{(w)} + 2e \qquad (4)$$
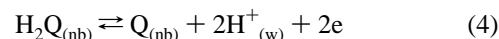
This overall reaction comprises the 2e/2H$^+$ redox transformation in the membrane and the expulsion of protons into the aqueous phase. It should be taken into account that water-saturated NB contains 0.2 mol/L water. Thus, it is plausible to assume that the protons can be accepted by the water molecules, and the charge neutrality of the membrane can be maintained by ingress of aqueous ClO$_4^-$ ions, which are present in a large excess in both liquid phases. Hence, the reaction 2 can be written as:

$$H_2Q_{(nb)} + 2ClO_4^-{}_{(w)} \rightleftharpoons Q_{(nb)} + 2H^+{}_{(nb)} + 2ClO_4^-{}_{(nb)} + 2e \qquad (5)$$
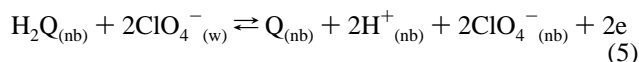
Taking into account the standard Gibbs energy for the transfer from water into NB of ClO$_4^-$ and H$^+$ (i.e., $\Delta^{w\rightarrow nb}G^\theta_{ClO_4^-} = 7.4$ kJ mol^{-1} and $\Delta^{w\rightarrow nb}G^\theta_{H^+} = 32.5$ kJ mol^{-1}),[26] the expulsion of protons from NB membrane is the thermodinamically favored process.

Kinetic measurements performed with QRM showed that the electrochemical process I was accelerated by increasing the concentration of the ClO$_4^-$ ion in the aqueous phase (cf. Figure 9). Recall that the Galvani potential difference at the membrane/water interface ($\Delta\phi^o_w$) ($\Delta\phi^o_w = \phi_o - \phi_w$; ϕ_o and ϕ_w are the inner potential of the membrane and aqueous phase, respectively) is defined as follows:

$$\Delta\phi^o_w = \Delta^{w\rightarrow o}\phi^\theta_{ClO_4^-} + \frac{RT}{F} \ln \frac{[ClO_4^-]_o}{[ClO_4^-]_w} \qquad (6)$$

Here $\Delta^{w\rightarrow o}\phi^\theta_{ClO_4^-}$ is the standard transfer potential of ClO$_4^-$ from water to NB, and [ClO$_4^-$] designates the equilibrium concentration. In addition, the partition concentration of protons in the organic phase depends on $\Delta\phi^o_w$ as follows:

$$[H^+]_o = [H^+]_w \exp\left[-\frac{F}{RT}(\Delta\phi^o_w - \Delta^{w\rightarrow o}\phi^\theta_{H^+})\right] \qquad (7)$$

where $\Delta^{w\rightarrow o}\phi^\theta_{H^+}$ is the standard transfer potential of H$^+$. For [ClO$_4^-$]$_o$ = 0.1 mol/L, increasing [ClO$_4^-$]$_w$ from 0.01 to 0.1 mol/L, as in Figure 9, caused $\Delta\phi^o_w$ to change from 137 to 80 mV, thereby enhancing the concentration of protons in the organic phase. This can finally cause an increase in the rate of the 2e/2H$^+$ redox transformation in the membrane. Thus, the conclusion of whether the redox transformation in the membrane or the proton expulsion is the rate-limiting step is not straightforward.

Results presented in Figures 10 and 11 reveal the binding affinity of H$_2$Q toward Ca^{2+} through an interfacial complexation reaction at the membrane/water interface. The consistent shift of both peaks I and II as a function of the Ca^{2+} concentration implies that both redox forms **1** and **2** are involved in the interfacial complexation (cf. Figure 10A), resulting in assisted

6076 *J. Phys. Chem. C, Vol. 111, No. 16, 2007*

Mirčeski et al.

transfer of Ca^{2+} ions in the membrane interior. Upon oxidation, Ca^{2+} ions are expelled out of the membrane. Both peak potentials shift equally with log $[Ca^{2+}]$ (cf. Figure 10B) and with a slope of about 30 mV, indicating formation of a complex with 1:1 stoichiometry. This is in agreement with the results of Bennet et al. who reported the stability constants of 820 and 75 mol^{-1} L for the complexes of one Ca^{2+} ion with one or two HQ^- ions, respectively.[10] The electrochemical reaction in the presence of Ca^{2+} ions can be represented by the following scheme:

$$CaHQ^+{}_{(nb)} + ClO_4{}^-{}_{(nb)} \rightleftarrows Q_{(nb)} + Ca^{2+}{}_{(w)} + H^+{}_{(w)} + \\ ClO_4{}^-{}_{(w)} + 2e \quad (8)$$
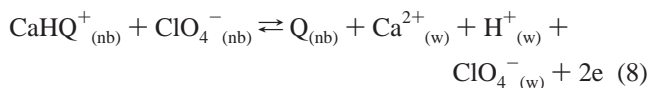
This equation clearly explains why the pH dependence of the peak potential is switched from -60 to -30 mV/pH in the absence and presence of Ca^{2+} ions, respectively.

The formation of the Ca^{2+} complex by engaging the two adjacent oxygen atoms of H_2Q molecule expels the proton (or protons) that is involved in the tautomerism equilibrium 1, thus preventing formation of the **2** form. As a consequence, in the presence of Ca^{2+} the equilibrium 1 is shifted strongly toward the form **1**, causing a substantial increase of the peak I over the peak II. This can be achieved by either subsequent cycling of the potential (cf. Figure 11A) or incubation of the electrode in the Ca^{2+}-containing solution under open circuit conditions (cf. Figure 11B).

The overall voltammetric behavior in the presence of Mg^{2+} (Figure 12A) is equivalent to that in the presence of Ca^{2+} ions, revealing that H_2Q does not discriminate between Ca^{2+} and Mg^{2+} ions. On the contrary, the voltammetric response is insensitive to Ba^{2+} (Figure 12B), showing the absence of complexing ability of H_2Q toward these ions that could be rationalized by taking the larger ionic radius of Ba^{2+} into account, which does not fit with the distance between the oxygen atoms participating in the complexation.

5. Conclusion

Controlling pH and Ca^{2+} concentrations within a certain range in the intra- and extracellular space of the human body are necessary for the proper function of all organs. Because organic compounds containing a benzoquinone/hydroquinone moiety are highly relevant for many physiological functions, we analyzed their redox, binding, and transport properties. Using SWV and CV, we found that H_2Q can be oxidized to a quinone form through $2e/2H^+$ redox pathway coupled by expulsion of protons out of the interior of the membrane. H_2Q undergoes two distinct oxidation processes with either yielding a quinone form. The two redox processes are assigned to two tautomer forms of H_2Q formed by migration of a proton between the hydroxyl group in the position 1 of the hydroquinone ring and the adjacent carbonyl group of the palmitoyl residue.

Taking further advantage of the quantitative and kinetic aspects of the data analysis, we could show how Ca^{2+} and proton binding and their transport by the quinone/hydroquinone system

interact with each other. The Ca^{2+} transport was found to be clearly pH dependent. The stoichiometry for Ca^{2+}/HQ^- is 1:1. Upon oxidation of the Ca^{2+}-H_2Q complex in the membrane, Ca^{2+} together with one proton are expelled out of the membrane. Whereas binding and transfer across membrane/water interface were found to be similar for Mg^{2+}, Ba^{2+} did not affect the voltammetric response. This indicates that the studied compound does not discriminate between Ca^{2+} and Mg^{2+}, the two physiologically relevant divalent cations, but can discriminate against other cations.

References and Notes

(1) Dallner, G.; Sindelar, P. J. *Free Radical Biol. Med.* **2000**, *29*, 285.

(2) Laviron, E. *J. Electroanal. Chem.* **1984**, *164*, 213.

(3) (a) Gordillo, C. J.; Schiffrin, D. J. *Faraday Discuss.* **2000**, *116*, 89. (b) Moncelli, M. R.; Becucci, L.; Nelson, A.; Guidelli, R. *Biophys. J.* **1996**, *70*, 2716.

(4) Gordillo, C. J.; Schiffrin, D. J. *J. Chem. Soc., Faraday Trans.* **1994**, *90*, 1913.

(5) Sek, S.; Bilewicz, R. *J. Inclusion Phenom. Macrocyclic Chem.* **1999**, *35*, 55.

(6) Mulkidjanian, A. Y.; Cherepanov, D. A.; Heberle, J.; Junge, W. *Biochemistry* **2005**, *70*, 251.

(7) Eckert, T. S.; Bruice, T. C.; Gainor, J. A.; Weinreb, S. M. *Proc. Natl. Acad. Sci. U.S.A.* **1982**, *79*, 2533.

(8) Itos, S.; Kawakami, H.; Fukuzumi, S. *J. Am. Chem. Soc.* **1998**, *120*, 7271.

(9) Zhou, J.; Felderhoff, M.; Smelkova, N.; Gornastaev, L. M.; Rieker, A. *J. Chem. Soc., Perkin Trans.* **1998**, *2*, 343.

(10) Bennett, I. M.; Vanegas Farfano, H. M.; Bogani, F.; Primak, A.; Liddell, P. A.; Otero, L.; Sereno, L.; Silber, J. J.; Moore, A. L.; Moore, T. A.; Gust, D. *Nature* **2002**, *420*, 398.

(11) Quintana, A.; Griesemer, D.; Schwarz, E. C.; Hoth, M. *Pflugers Arch.* **2005**, *450*, 1.

(12) Chung, T. D.; Anson, F. C. *Anal. Chem.* **2001**, *73*, 337.

(13) Shi, C. N.; Anson, F. C. *Anal. Chem.* **1998**, *70*, 3114.

(14) Shi, C. N.; Anson, F. C. *J. Phys. Chem. B* **1998**, *102*, 9850.

(15) Scholz, F.; Gulaboski, R. *ChemPhysChem* **2005**, *6*, 16.

(16) Mirčeski, V.; Quentel, F.; L'Her, M.; Pondaven, A. *Electrochem. Commun.* **2005**, *7*, 1122.

(17) Mirčeski, V.; Quentel, F.; L'Her, M.; Scholz, F. *J. Electroanal. Chem.* **2006**, *586*, 86.

(18) Gulaboski, R.; Mirčeski, V.; Pereira, C. M.; Cordeiro, M. N. D. S.; Silva, A. F.; Quentel, F.; L'Her, M.; Lovrić, M. *Langmuir* **2006**, *22*, 3404.

(19) Marken, F.; Neudeck, A.; Bond, A. M. Cyclic Voltammetry. In *Electroanalytical Methods*; Scholz, F., Ed.; Springer: Berlin, 2001; pp 50−97.

(20) Lovric, M. Square-Wave Voltammetry. In *Electroanalytical Methods*; Scholz, F., Ed.; Springer: Berlin, 2001; p 111.

(21) Mirčeski, V. *J. Phys. Chem. B* **2004**, *108*, 13719.

(22) Quentel, F.; Mirčeski, V.; L'Her, M. *Anal. Chem.* **2005**, *77*, 1940.

(23) Laviron, E. *J. Electroanal. Chem.* **1984**, *164*, 213.

(24) Chi, Y.; Duan, J.; Qi, X.; Chen, G. *Bioelectrochemistry* **2003**, *60*, 37.

(25) Vollhardt, K. P. C.; Schore N. E. *Organische Chemie*, 3rd edition; Wiley: Weinheim, 2000; pp 843−846.

(26) ElectroChemical Data Base. http://lepa.epfl.ch/.